THREE-BODY MODEL FOR NUCLEI NEAR AND BEYOND DRIP LINE*

Hiroyuki Sagawa

RIKEN Nishina Center, Wako 351-0198, Japan
and
Center for Mathematics and Physics, University of Aizu
Aizu-Wakamatsu, Fukushima 965-8560, Japan

Kouichi Hagino

Department of Physics, Tohoku University, Sendai 980-8578, Japan
and
Research Center for Electron Photon Science, Tohoku University
Sendai 982-0826, Japan
and
National Astronomical Observatory of Japan
2-21-1 Osawa, Mitaka, Tokyo 181-8588, Japan

We discuss firstly possible experimental probes for the strong di-neutron correlations in halo nuclei ^{6}He and ^{11}Li. We then secondly study a nucleus beyond the drip line ^{26}O through the direct two-neutron decay. The excites 2^+ state of ^{26}O is also discussed. We use consistently a three-body model to this end, taking into account the coupling to the continuum. Calculated results are compared with the recent experimental data from RIBF (Radioactive Ion Beam Factory) in RIKEN.

1. Introduction

One of the most important issues in many-body physics is to clarify the nature of correlations beyond the independent particle picture. In nuclear physics, the pairing correlation has been well-recognized as a typical many-body correlation which leads to the phase of superfluidity characterized by

---

phenomena such as the even–odd staggering of binding energy, the moment of inertia of rotating deformed nuclei and the difference of the excitation energy spectra between even–even and odd–even nuclei [1–3].

With the pairing correlation, one may naively expect that two nucleons forming a pair are located at a similar position inside a nucleus. A spatial structure of two valence neutrons has, in fact, attracted much attention in the past. One of the oldest publications on this problem is by Bertsch, Broglia, and Riedel, who solved a shell model for ^{210}Pb and showed that the two valence neutrons are strongly clusterized [4]. Subsequently, Migdal argued that two neutrons may be bound in a nucleus even though they are not bound in the vacuum [5].

The strong localization of two neutrons inside a nucleus has been referred to as the *di-neutron correlation*. It has been nicely demonstrated in Ref. [6] that an admixture of configurations of single-particle orbits with opposite parity is essential to create the strong di-neutron correlation. This implies that the pairing correlation acting only on single-particle orbits with the same parity may not be sufficient in order to develop the di-neutron correlation, and the pairing model space needs to be taken sufficiently large so that both positive parity and negative parity states are included.

Although the di-neutron correlation exists even in stable nuclei, it is, therefore, more enhanced in weakly bound nuclei because the admixtures of single-particle orbits with different parities are easier due to the couplings to the continuum spectra [7, 8]. Three-body model calculations have revealed that a strong di-neutron correlation indeed exists in weakly-bound Borromean nuclei, such as ^{11}Li and ^{6}He [9–14]. For instance, Fig. 1 shows the two-particle density for the ^{11}Li and ^{6}He nuclei obtained with the three-body model calculation with a density-dependent contact pairing interaction [12]. One can see that the densities are concentrated in the region with
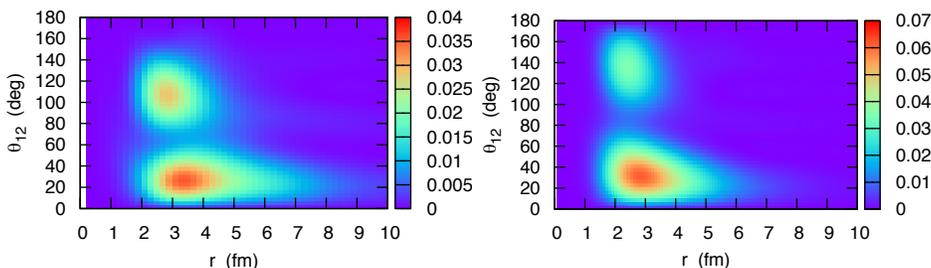

Fig. 1. The two-particle densities for ^{11}Li (the left panel) and for ^{6}He (the right panel) obtained with a three-body model calculation with a density-dependent contact pairing interaction [12]. These are plotted as a function of neutron–core distance, $r_1 = r_2 \equiv r$, and the opening angle between the valence neutrons, θ_{12}. The densities are weighted with a factor $8\pi^2 r^4 \sin\theta_{12}$.

small opening angles, that is nothing but the di-neutron correlation. It has been shown that the di-neutron correlation exists also in heavier neutron-rich nuclei [15, 16] as well as in infinite neutron matter [17]. The di-proton correlation, which is a counter part of the di-neutron correlation, has also been shown to exist in the proton-rich Borromean nucleus, [17]Ne [18].

From these studies, the di-neutron correlation seems to have been theoretically established. However, it is not straightforward to probe it experimentally. In this contribution, we discuss how one can probe the di-neutron correlation. To be more specific, we shall discuss the Coulomb breakup, and the two-nucleon radioactivity as prominent probes for the correlation.

2. Electric dipole strength of Borromean nuclei and di-neutron correlations

Let us first discuss the Coulomb breakup reactions of Borromean nuclei, [11]Li and [6]He, for which the experimental data have been available in Refs. [19,20]. Those experimental breakup cross sections, especially those for the [11]Li nucleus, show a strong concentration in the low excitation region, reflecting the halo structure of these nuclei. Moreover, the experimental data for [11]Li are consistent only with the theoretical calculation which takes into account the interaction between the valence neutrons, strongly suggesting the existence of the di-neutron correlation in this nucleus (see also Ref. [21]).

For the Coulomb breakup of Borromean nuclei, one can go one step further, given that the Coulomb breakup process takes place predominantly by the dipole excitation. The Coulomb breakup cross sections with the absorption of dipole photons are given by

$$\frac{\mathrm{d}\sigma_\gamma}{\mathrm{d}E_\gamma} = \frac{16\pi^3}{9\hbar c} N_\gamma(E_\gamma) \frac{\mathrm{d}B(\mathrm{E1})}{\mathrm{d}E_\gamma} \,, \tag{1}$$

where N_γ is the number of virtual photons, and

$$\frac{\mathrm{d}B(\mathrm{E1})}{\mathrm{d}E_\gamma} = \frac{1}{2I_\mathrm{i}+1} \left|\langle\psi_\mathrm{f}||D||\psi_\mathrm{i}\rangle\right|^2 \delta\left(E_\mathrm{f} - E_\mathrm{i} - E_\gamma\right) \tag{2}$$

is the reduced E1 transition probability. In this equation, ψ_i and ψ_f are the wave functions for the initial and the final states, respectively, I_i is the spin of the initial state, and D_μ is the operator for the E1 transition. For the Borromean nuclei, assuming a three-body structure with an inert core, the E1 operator D_μ reads [22],

$$\hat{D}_\mu = \frac{e_{\mathrm{E1}}}{2} \left(r_1 Y_{1\mu}\left(\hat{\vec{r}}_1\right) + r_2 Y_{1\mu}\left(\hat{\vec{r}}_2\right)\right) \,, \tag{3}$$

where the E1 effective charge is given by

$$e_{\mathrm{E1}} = \frac{2Z_{\mathrm{c}}}{A_{\mathrm{c}} + 2}\, e\,, \tag{4}$$

with A_{c} and Z_{c} being the mass and charge numbers for the core nucleus. The dipole transition of di-neutrons is entirely the recoil effect of protons in the core and the center-of-mass motion is exactly removed from the dipole operator (3). Experimental data of the transition probabilities (2) are shown in Fig. 2 with results calculated by a three-body model in Ref. [21]. We can see clearly a strong enhancement of $B(\mathrm{E1})$ strength just above the threshold energy due to the di-neutron correlations.
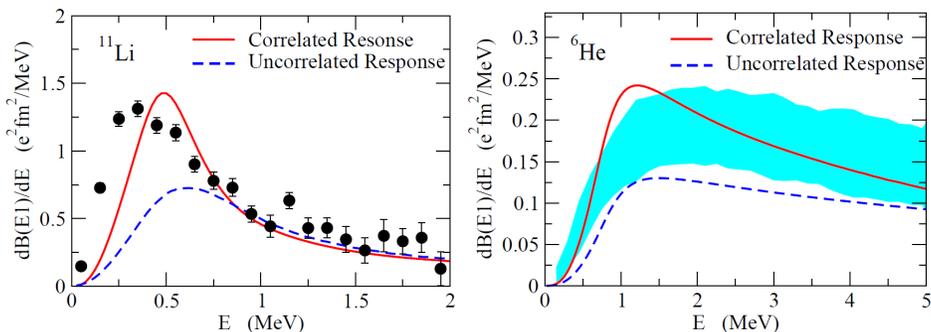

Fig. 2. (Color online) The eltric dipole transitions in ^{11}Li and ^{6}He observed by the Coulomb breakup reactions. The data are taken from Ref. [19] for ^{11}Li and from Ref. [20] for ^{6}He, respectively.

Using Eq. (2) and the closure relation for the final state, it is easy to derive that the total E1 strength (that is, the non-energy weighted sum rule) is proportional to the expectation value of R^2 with respect to the ground state, that is,

$$B(\mathrm{E1}) = \int \mathrm{d}E_{\gamma} \frac{\mathrm{d}B(\mathrm{E1})}{\mathrm{d}E_{\gamma}} = \sum_{f} \frac{1}{2I_{\mathrm{i}} + 1} |\langle\psi_{\mathrm{f}}||D||\psi_{\mathrm{i}}\rangle|^2 = \frac{3}{4\pi} e_{\mathrm{E1}}^2 \left\langle \vec{R}^2 \right\rangle\,, \tag{5}$$

where

$$\vec{R} = \frac{\vec{r}_1 + \vec{r}_2}{2} \tag{6}$$

is the center-of-mass coordinate for the two valence neutrons. Even though the $B(\mathrm{E1})$ strength distribution inevitably reflects both the correlation in the ground state and that in the final state, it is remarkable that one can extract the information which reflects *solely* the ground state properties after summing all the strength distribution. This implies that the average value

of the opening angle between the valence neutrons can be directly extracted from the measured total $B(E1)$ value once the root-mean-square distance between the valence neutrons, $\langle r_{nn}^2 \rangle$, is available (see Fig. 3).
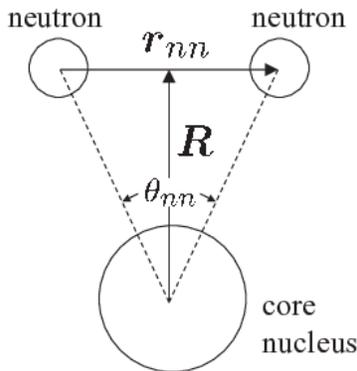

Fig. 3. The geometry of a $2n$ halo nucleus consisting of a core nucleus and two valence neutrons.

This quantity is related to the matter radius and $\langle R^2 \rangle$ in the three-body model [9, 21, 23]

$$\langle r_{\mathrm{m}}^2 \rangle = \frac{A_{\mathrm{c}}}{A} \langle r_{\mathrm{m}}^2 \rangle_{A_{\mathrm{c}}} + \frac{2A_{\mathrm{c}}}{A^2} \langle R^2 \rangle + \frac{1}{2A} \langle r_{nn}^2 \rangle \,, \tag{7}$$

where $A = A_{\mathrm{c}} + 2$ is the mass number of the whole nucleus. The matter radii $\langle r_{\mathrm{m}}^2 \rangle$ can be estimated from interaction cross sections. Employing the Glauber theory in the optical limit, Tanihata *et al.* have obtained $\sqrt{\langle r_{\mathrm{m}}^2 \rangle} = 1.57\pm0.04$, 2.48 ± 0.03, 2.32 ± 0.02, and 3.12 ± 0.16 fm for ^{4}He, ^{6}He, ^{9}Li, and ^{11}Li, respectively [24, 25]. Using these values, we obtain the r.m.s. neutron–neutron distance of $\sqrt{\langle r_{nn}^2 \rangle} = 3.75 \pm 0.93$ and 5.50 ± 2.24 fm for ^{6}He and ^{11}Li, respectively. Combining these values with the r.m.s. core–di-neutron distance, $\sqrt{\langle R^2 \rangle}$, we obtain the mean opening angle

$$\langle \theta_{nn} \rangle = 2 \tan^{-1} \left(\sqrt{\langle r_{nn}^2 \rangle} / 2\sqrt{\langle R^2 \rangle} \right) \tag{8}$$

to be $51.56^{+11.2}_{-12.4}$ and $56.2^{+17.8}_{-21.3}$ degrees for ^{6}He and ^{11}Li, respectively [26]. These values are comparable to the result of the three-body model calculation, $\langle \theta_{nn} \rangle = 66.33$ and 65.29 degree for ^{6}He and ^{11}Li, respectively [12], although the experimental values are somewhat smaller.

An alternative way to extract the value for $\sqrt{\langle r_{nn}^2 \rangle}$ which uses the three-body correlation study in the dissociation of two neutrons in halo nuclei has been proposed [27]. The two-neutron correlation function provides the

experimental values for $\sqrt{\langle r_{nn}^2 \rangle}$ to be 5.9 ± 1.2 and 6.6 ± 1.5 fm for ^{6}He, ^{11}Li, respectively [27]. Bertulani and Hussein used these values to estimate the mean opening angles and obtained $\langle \theta_{nn} \rangle = 83^{+20}_{-10}$ and 66^{+22}_{-18} degrees for ^{6}He and ^{11}Li, respectively [28]. After correcting the effect of Pauli forbidden transitions using the method presented in Ref. [21], these values are slightly altered to be $\langle \theta_{nn} \rangle = 74.5^{+11.2}_{-13.1}$ and $65.2^{+11.4}_{-13.0}$ degrees for ^{6}He and ^{11}Li, respectively [26]. Notice that these values are in better agreement with the results of the three-body calculation [12], especially for the ^{6}He nucleus.

In the absence of the correlations, the mean opening angle is exactly $\langle \theta_{nn} \rangle = 90$ degrees. The extracted values of $\langle \theta_{nn} \rangle$ are significantly smaller than this value both for ^{11}Li and ^{6}He, providing a direct proof of the existence of the di-neutron correlation in these nuclei. A small drawback is that this method provides only the average value of $\langle \theta_{nn} \rangle$ and a detailed distribution is inaccessible. In reality, the mean opening angle is most probably an average of a smaller and a larger correlation angles in the density distribution, as has been shown in Fig. 1.

3. Two-neutron decays of nuclei beyond the drip lines

3.1. The ground state of ^{26}O

In the Coulomb breakup process discussed in Sec. 2, the ground state wave function of a two-neutron halo nucleus is firstly perturbed by the external electromagnetic field of the target nucleus. It may thus not be easy to disentangle the di-neutron correlation in the ground state from that in the excited states. The two-proton radioactivity, that is, a spontaneous emission of two valence protons, of proton-rich nuclei [29] is expected to provide a good tool to probe the di-proton correlation in the initial wave function. An attractive feature of this phenomenon is that the two valence protons are emitted directly from the ground state even without any external perturbation.

Very recently, the ground state *two-neutron* emissions have also been observed, *e.g.* in ^{10}He [30–34], ^{16}Be [35], ^{13}Li [32,36], and ^{26}O [37–40]. This is an analogous process of the two-proton radioactivity, corresponding to a penetration of two neutrons over a centrifugal barrier. Since the long range Coulomb interaction is absent, one may hope that the ground state correlation can be better probed by studying the energy and the angular correlations of the emitted neutrons, as compared to the two-proton decays.

Figure 4 shows the calculated decay energy spectrum of ^{26}O obtained with the ^{24}O$+n+n$ three-body model for ^{26}O [44]. The calculations are carried out using the Green's function method as explained in Refs. [8,22,41,42], together with a density-dependent contact neutron–neutron interaction, v.

In this formalism, the decay energy spectrum is given by

$$\frac{\mathrm{d}P}{\mathrm{d}E} = \sum_k |\langle \Psi_k | \Phi_{\mathrm{ref}} \rangle|^2 \, \delta(E - E_k) = \frac{1}{\pi} \Im \langle \Phi_{\mathrm{ref}} | G(E) | \Phi_{\mathrm{ref}} \rangle \,, \tag{9}$$

where Ψ_k is a solution of the three-body model Hamiltonian with energy E_k and Φ_{ref} is the wave function for a reference state. The reference state can be taken rather arbitrarily as long as it has an appreciable overlap with the resonance states of interest. Here, we employ the uncorrelated two-neutron state in ^{27}F for it with the $|[1d_{3/2} \otimes 1d_{3/2}]^{(I=0)}\rangle$ configuration, which is the dominant configuration in the initial state of the proton knockout reaction of ^{27}F to produce ^{26}O. In Eq. (9), G is the correlated two-particle Green's function calculated as

$$G(E) = (1 + G_0(E)v)^{-1} G_0(E) = G_0(E) - G_0(E)v(1 + G_0(E)v)^{-1} G_0(E) \,, \tag{10}$$

with the uncorrelated Green's function, G_0, given by

$$G_0(E) = \lim_{\eta \to 0} \sum_{1,2} \!\!\!\!\!\!\! \int \frac{|j_1 j_2\rangle \langle j_1 j_2|}{\epsilon_1 + \epsilon_2 - E - i\eta} \,, \tag{11}$$

where η is an infinitesimal number and the sum includes all independent two-particle states including both the bound and the continuum single-particle states. In Eq. (10), v is the two-body interaction between two neutrons. To calculate the single-particle energies, we use the Woods–Saxon potential for the neutron-^{24}O potential which reproduces the experimental single-particle energies of $\epsilon_{2s_{1/2}} = -4.09(13)$ MeV and $\epsilon_{1d_{3/2}} = 749(10)$ keV for ^{25}O [39]. The parameters for the density-dependent zero-range pairing interaction are determined so as to yield the decay energy of 18 keV.

In the figure, we show the spectrum for the uncorrelated case by the dotted line. In this case, the spectrum has a peak at $E = 1.498$ MeV, that is twice the single-particle resonance energy, 0.749 MeV. With the pairing interaction between the valence neutrons, the peak energy is shifted towards lower energies. The decay spectrum obtained by including only the $[d_{3/2}]^2$ configurations is shown by the dashed line. In this case, the peak is shifted by 0.55 MeV from the unperturbed peak at 1.498 MeV. The peak is further shifted downwards by the di-neutron correlations due to configuration mixing, and gets closer to the threshold energy. This comparison implies that the pairing correlation for the single configuration is not enough to reproduce the empirical decay spectrum, and the di-neutron correlations between the two neutrons also play an essential role.
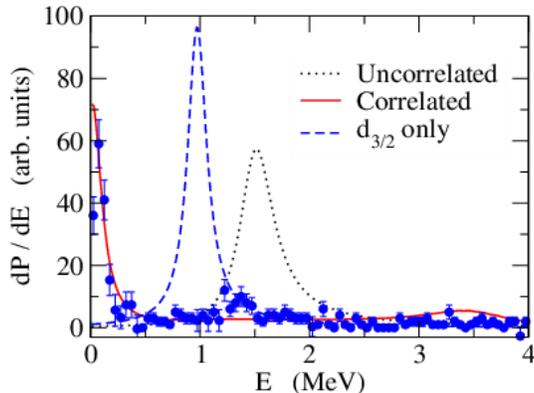
Fig. 4. The decay energy spectrum for the two-neutron emission decay of ^{26}O, obtained with the ^{24}O+n+n three-body model. For the presentation purpose, a width of 0.1 MeV has been introduced to the spectrum. The dotted line is for the uncorrelated spectrum, while the solid line shows the correlated spectrum for the 0^+ state. The dashed line shows the spectrum obtained by including the pairing correlation only for the $[d_{3/2}]^2$ configuration. The experimental data are taken from Ref. [39].

3.2. The first excited state

Let us next discuss the first 2^+ state in ^{26}O. One of the most important findings in the recent experiment reported in Ref. [39] is a finding of a clear second peak at $E = 1.28^{+0.11}_{-0.08}$ MeV, which is likely attributed to the 2^+ state. In Refs. [42, 44], we have investigated the 2^+ state in the ^{26}O nucleus using the three-body model. That is, the energy spectrum for this state can be obtained with the Green's function approach, by using a 2^+ state for the reference state, Φ_{ref}, as well as in the unperturbed Green's function, Eq. (11) [42]. Due to the pairing interaction between the valence neutrons, the energy of the 2^+ state is slightly shifted towards lower energies from the unperturbed energy, whereas the energy shift is much larger for the 0^+ state due to the larger overlap between the wave functions of the two neutrons. The 2^+ peak appears at 1.282 MeV, which agrees perfectly with the experimental data [44].

While we achieve an excellent agreement with the experimental data for the energy of the 2^+ state, it is striking to notice that most of theoretical calculations performed so far overestimate the energy. For instance, an *ab initio* calculation with chiral NN and $3N$ interactions predicts E_{2^+} to be 1.6 MeV above the ground state [45]. Shell model calculations with the USDA and USDB interactions [46] yield E_{2^+} to be 1.9 and 2.1 MeV, respectively [45], whereas the continuum shell model calculations predict the excitation energy

of 1.8 MeV [47] and 1.66 MeV [48]. The recent three-body model calculation
by Grigorenko and Zhukov shows the energy to be 1.6 MeV [49]. We sum-
marize these results in Table I together with the energy of the $3/2^+$ state
in ^{25}O for each calculation. It is not clear what causes these overestimates
of the 2^+ energy, but the 2^+ state should certainly appear at an energy
slightly lower than the unperturbed state, as long as the three-body struc-
ture is reasonable. In this sense, the *ab initio* calculation with chiral NN
and $3N$ interactions shows the opposite trend, and the shell model calcu-
lations, except for the continuum shell model calculations of Refs. [47, 48],
seem to overestimate the correlation (unfortunately, we cannot judge this for
the recent three-body model calculation of Grigorenko and Zhukov, because
they do not discuss the energy of the ^{25}O nucleus and also because the exact
form of the spin-orbit form which they employ is not clear).

<div align="right">TABLE I</div>

Comparison of the energies of the $3/2^+$ state of ^{25}O and the 2^+ state of ^{26}O
obtained with several methods. These values, given in units of MeV, are measured
from the thresholds.

Method	^{25}O $(3/2^+)$	^{26}O (2^+)	Reference
Shell model (USDA)	1.301	1.9	[45]
Shell model (USDB)	1.303	2.1	[45]
Chiral $NN + 3N$	0.742	1.64	[45]
Continuum shell model	1.002	1.8	[47]
Continuum-coupled shell model	0.86	1.66	[48]
3-body model	—	1.6	[49]
3-body model	0.749 (input)	1.282	this work
Experiment	0.749 (10)	$1.28^{+0.11}_{-0.08}$	[39]

3.3. The angular distributions of emitted neutrons

The angular distribution of the emitted neutrons can also be calculated
with the two-particle Green's function method [22, 41, 44]. The amplitude
for emitting two neutrons with spin components of s_1 and s_2, and momenta
$\vec{k}_1$ and $\vec{k}_2$ reads [41]

$$f_{s_1 s_2}\left(\vec{k}_1, \vec{k}_2\right) = \sum_{j,l} e^{-il\pi} e^{i(\delta_1 + \delta_2)} M_{j,l,k_1,k_2} \left\langle \left[\mathcal{Y}_{jl}\left(\hat{\vec{k}}_1\right) \mathcal{Y}_{jl}\left(\hat{\vec{k}}_2\right)\right]^{(00)} \middle| \chi_{s_1} \chi_{s_2} \right\rangle,$$
(12)

where $\mathcal{Y}_{jlm}$ is the spin-spherical harmonics, χ_s is the spin wave function,
and δ is the nuclear phase shift. Here, M is a decay amplitude calculated to

a specific two-particle final state [22]

$$M_{j,l,k_1,k_2} = \langle (jj)^{(00)}|1-vG_0+vG_0vG_0-\cdots|\Psi_i\rangle = \langle (jj)^{(00)}|(1+vG_0)^{-1}|\Psi_i\rangle \,, \tag{13}$$

where the unperturbed Green's function, G_0, is evaluated at $E = e_1 + e_2$. The angular distribution is then obtained as

$$P(\theta_{12}) = 4\pi \sum_{s_1,s_2} \int \mathrm{d}k_1\mathrm{d}k_2 \left| f_{s_1s_2}\left(k_1, \hat{\vec{k}}_1 = 0, k_2, \hat{\vec{k}}_2 = \theta_{12}\right)\right|^2 \,, \tag{14}$$

where we have set z-axis to be parallel to $\vec{k}_1$ and evaluated the angular distribution as a function of the opening angle, θ_{12}, of the two emitted neutrons.

Figure 5 shows the so obtained angular correlation. The dot-dashed line shows the distribution obtained without including the nn interaction, which is symmetric around $\theta_{12} = \pi/2$. In the presence of the nn interaction, the angular distribution turns to be highly asymmetric and the emission of two neutrons in the opposite direction (that is, $\theta_{12} = \pi$) is enhanced, as is shown by the solid line. Grigorenko *et al.* [50] have also obtained a similar result.
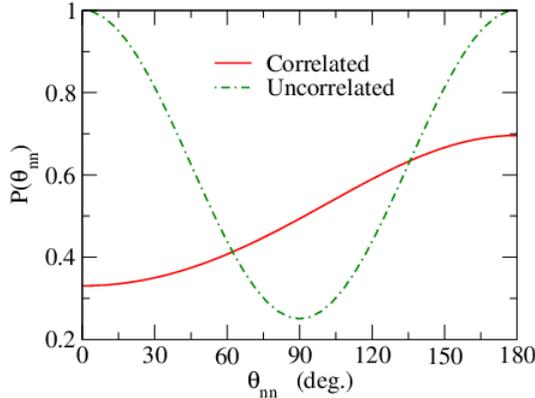

Fig. 5. The angular correlation for the two emitted neutrons from the ground state decay of ^{26}O. The probability distribution for the opening angle of the momentum vectors of the emitted neutrons is shown. The solid and the dot-dashed lines denote the correlated and uncorrelated results, respectively.

This behavior reflects properties of the resonance wave function of ^{26}O. That is, because of the continuum couplings, several configurations with opposite parity states mix coherently. Symbolically, let us write a two-particle wave function as

$$\Psi\left(\vec{r},\vec{r}'\right) = \alpha\,\Psi_{\mathrm{ee}}\left(\vec{r},\vec{r}'\right) + \beta\,\Psi_{\mathrm{oo}}\left(\vec{r},\vec{r}'\right) \,, \tag{15}$$

where Ψ_{ee} and Ψ_{oo} are two-particle wave functions with even and odd angular momentum states, respectively. The coefficients α and β are such that the interference term in the two-particle density, $\alpha^*\beta\Psi_{\text{ee}}^*\Psi_{\text{oo}} + \text{c.c.}$, is positive for $\vec{r}\,' = \vec{r}$, while it is negative for $\vec{r}\,' = -\vec{r}$ so that the two-particle density is enhanced for the nearside configuration with $\vec{r} \sim \vec{r}\,'$ as compared to the far side configuration with $\vec{r} \sim -\vec{r}\,'$. This correlation appears in the opposite way in the momentum space. In the Fourier transform of $\Psi(\vec{r}, \vec{r}\,')$,

$$\widetilde{\Psi}\left(\vec{k}, \vec{k}\,'\right) = \int d\vec{r} d\vec{r}\,'\, e^{i\vec{k}\cdot\vec{r}} e^{i\vec{k}\,'\cdot\vec{r}\,'}\, \Psi\left(\vec{r}, \vec{r}\,'\right)\,, \tag{16}$$

there is a factor i^l in the multipole decomposition of $e^{i\vec{k}\cdot\vec{r}}$. Since $\left(i^l\right)^2$ is $+1$ for even values of l and -1 for odd values of l, this leads to [8, 41]

$$\widetilde{\Psi}\left(\vec{k}, \vec{k}\,'\right) = \alpha\,\widetilde{\Psi}_{\text{ee}}\left(\vec{k}, \vec{k}\,'\right) - \beta\,\widetilde{\Psi}_{\text{oo}}\left(\vec{k}, \vec{k}\,'\right) \tag{17}$$

for the two particle wave function given by Eq. (15). If one constructs a two-particle density in the momentum space with this wave function, the interference term acts, therefore, in the opposite way to that in the coordinate space. That is, the two-particle density in the momentum space is hindered for $\vec{k} \sim \vec{k}'$, while it is enhanced for $\vec{k} \sim -\vec{k}'$. This feature can be also understood by the argument of Heisenberg uncertainty principle, *i.e.*, a strong correlation in the coordinate space (a small value of $\Delta r = |\vec{r}\,' = \vec{r}|$) corresponds to a back-to-back correlation in the momentum space (a large value of $\Delta p = \hbar\Delta k = \hbar|\vec{k}' = \vec{k}|$). From this argument, we can, therefore, conclude that, if an enhancement in the region of $\theta \sim \pi$ in the angular distribution was observed experimentally, that would make a clear evidence for the di-neutron correlation in this nucleus, although such measurement will be experimentally challenging [51].

Incidentally, the tunneling decay of two fermionic ultracold atoms has been measured very recently [52] (see also Ref. [53] for an application of the Gamow shell model to this phenomenon). An attractive feature of this experiment is that several parameters are experimentally controllable, which include the sign and the strength of the interaction between the particles and the shape of a decaying potential. It may be useful to carry out in future detailed analyses of the tunneling decay of ultracold atoms in order to shed light on the two-proton and two-neutron decay problems in nuclear physics.

4. Summary

We have discussed possible experimental probes for the di-neutron correlation in neutron-rich nuclei, with which two valence nucleons are located at a similar position in the coordinate space. In particular, we have discussed the Coulomb dissociation of Borromean nuclei, and the direct two-neutron decay of the unbound ^{26}O nucleus.

For the Coulomb dissociation of Borromean nuclei, even though the detailed distribution is difficult to extract, one can use the cluster sum rule (that is, the non-energy weighted sum rule) to deduce the mean value of the opening angle between the valence neutrons. We have demonstrated that the mean opening angle is $\langle \theta_{nn} \rangle = 74.5^{+11.2}_{-13.1}$ and $65.2^{+11.4}_{-13.0}$ degrees for ^{6}He and ^{11}Li, respectively. These values are significantly smaller than the value for the uncorrelated distribution, that is, $\langle \theta_{nn} \rangle = 90$ degrees, clearly indicating the existence of the di-neutron correlation in these Borromean nuclei.

For the direct two-neutron decay, we have discussed the recent experimental data of the decay energy spectrum for the unbound ^{26}O nucleus. We have shown that the decay energy spectrum can be accounted for only with the di-neutron correlation due to the mixing of many configurations including the continuum. We have also discussed the angular correlations of the emitted two neutrons. We have argued that the di-neutron correlation enhances an emission of the two neutrons in the opposite direction (that is, the back-to-back emission) and, indeed, our three-body model calculation has revealed such feature. If the enhancement of the back-to-back emission will be observed experimentally, it will thus provide a direct evidence for the di-neutron correlation.

Even though we did not discuss them in this paper, there are other possible probes for the di-neutron correlation. Those include the two-neutron transfer reactions, the nuclear breakup reaction [54], the (p, d) scattering at backward angles [55, 56], and the knockout reactions of Borromean nuclei [57–60]. It would be extremely intriguing if the clear and direct evidence for the di-neutron correlation could be experimentally obtained in near future using also these probes.

REFERENCES

[1] A. Bohr, B.R. Mottelson, *Nuclear Structure Vol. 1*, World Scientific, Singapore 1975.

[2] P. Ring, P. Schuck, *The Nuclear Many Body Problem*, Springer-Verlag, New York 1980.

[3] D.M. Brink, R.A. Broglia, *Nuclear Superfluidity: Pairing in Finite Systems*, Cambridge University Press, Cambridge 2005.

[4] G.F. Bertsch, R.A. Broglia, C. Riedel, *Nucl. Phys. A* **91**, 123 (1967).

[5] A.B. Migdal, *Sov. J. Nucl. Phys.* **16**, 238 (1973).

[6] F. Catara, A. Insolia, E. Maglione, A. Vitturi, *Phys. Rev. C* **29**, 1091 (1984).

[7] K. Hagino, I. Tanihata, H. Sagawa, *Exotic Nuclei Far From the Stability Line*, in: E.M. Henley, S.D. Ellis (eds.), *100 Years of Subatomic Physics*, World Scientific, Singapore 2013, pp. 231–272.

[8] H. Sagawa, K. Hagino, *Eur. Phys. J. A* **51**, 102 (2015).

[9] G.F. Bertsch, H. Esbensen, *Ann. Phys. (N.Y.)* **209**, 327 (1991).

[10] M.V. Zhukov *et al.*, *Phys. Rep.* **231**, 151 (1993).

[11] F. Barranco *et al.*, *Eur. Phys. J. A* **11**, 385 (2001).

[12] K. Hagino, H. Sagawa, *Phys. Rev. C* **72**, 044321 (2005).

[13] K. Hagino, H. Sagawa, J. Carbonell, P. Schuck, *Phys. Rev. Lett.* **99**, 022506 (2007).

[14] Y. Kikuchi *et al.*, *Phys. Rev. C* **81**, 044308 (2010).

[15] M. Matsuo, K. Mizuyama, Y. Serizawa, *Phys. Rev. C* **71**, 064326 (2005).

[16] N. Pillet, N. Sandulescu, P. Schuck, *Phys. Rev. C* **76**, 024310 (2007).

[17] M. Matsuo, *Phys. Rev. C* **73**, 044309 (2006).

[18] T. Oishi, K. Hagino, H. Sagawa, *Phys. Rev. C* **82**, 024315 (2010).

[19] T. Nakamura *et al.*, *Phys. Rev. Lett.* **96**, 252502 (2006).

[20] T. Aumann *et al.*, *Phys. Rev. C* **59**, 1252 (1999).

[21] H. Esbensen, K. Hagino, P. Mueller, H. Sagawa, *Phys. Rev. C* **76**, 024302 (2007).

[22] H. Esbensen, G.F. Bertsch, *Nucl. Phys. A* **542**, 310 (1992).

[23] N. Vinh Mau, J.C. Pacheco, *Nucl. Phys. A* **607**, 163 (1996).

[24] I. Tanihata *et al.*, *Phys. Rev. Lett.* **55**, 2676 (1985).

[25] A. Ozawa *et al.*, *Nucl. Phys. A* **693**, 32 (2001).

[26] K. Hagino, H. Sagawa, *Phys. Rev. C* **76**, 047302 (2007).

[27] F.M. Marques *et al.*, *Phys. Lett. B* **476**, 219 (2000).

[28] C.A. Bertulani, M.S. Hussein, *Phys. Rev. C* **76**, 051602(R) (2007).

[29] M. Pfützner, M. Karny, L.V. Grigorenko, K. Riisager, *Rev. Mod. Phys.* **84**, 567 (2012).

[30] M.S. Golovkov *et al.*, *Phys. Lett. B* **672**, 22 (2009).

[31] H.T. Johansson *et al.*, *Nucl. Phys. A* **842**, 15 (2010).

[32] H.T. Johansson *et al.*, *Nucl. Phys. A* **847**, 66 (2010).

[33] S.I. Sidordhuk *et al.*, *Phys. Rev. Lett.* **108**, 202502 (2012).

[34] Z. Kohley *et al.*, *Phys. Rev. Lett.* **109**, 232501 (2012).

[35] A. Spyrou *et al.*, *Phys. Rev. Lett.* **108**, 102501 (2012).

[36] Z. Kohley *et al.*, *Phys. Rev. Lett.* **87**, 011304(R) (2013).

[37] E. Lunderberg *et al.*, *Phys. Rev. Lett.* **108**, 142503 (2012).

[38] C. Caesar *et al.*, *Phys. Rev. C* **88**, 034313 (2013).

[39] Y. Kondo *et al.*, *Phys. Rev. Lett.* **116**, 102503 (2016).

[40] Z. Kohley *et al.*, *Phys. Rev. Lett.* **110**, 152501 (2013).

[41] K. Hagino, H. Sagawa, *Phys. Rev. C* **90**, 027303 (2014).

[42] K. Hagino, H. Sagawa, *Phys. Rev. C* **90**, 027303 (2014).

[43] C.R. Hoffman *et al.*, *Phys. Rev. Lett.* **100**, 152502 (2008).

[44] K. Hagino, H. Sagawa, *Phys. Rev. C* **93**, 034330 (2016).

[45] C. Caesar *et al.*, *Phys. Rev. C* **88**, 034313 (2013).

[46] B.A. Brown, W.A. Richter, *Phys. Rev. C* **74**, 034315 (2006).

[47] A. Volya, V. Zelevinsky, *Phys. Rev. C* **74**, 064314 (2006).

[48] K. Tsukiyama, T. Otsuka, R. Fujimoto, *Prog. Theor. Exp. Phys.* **2015**, 093D01 (2015).

[49] L.V. Grigorenko, M.V. Zhukov, *Phys. Rev. C* **91**, 064617 (2015).

[50] L.V. Grigorenko, I.G. Mukha, M.V. Zhukov, *Phys. Rev. Lett.* **111**, 042501 (2013).

[51] Z. Kohley *et al.*, *Phys. Rev. C* **91**, 034323 (2015).

[52] G. Zürn *et al.*, *Phys. Rev. Lett.* **111**, 175302 (2013).

[53] R. Lundmark, C. Forssen, J. Rotureau, *Phys. Rev. A* **91**, 041601(R) (2015).

[54] M. Assie *et al.*, *Eur. Phys. J. A* **42**, 441 (2009).

[55] W. Horiuchi, Y. Suzuki, *Phys. Rev. C* **76**, 024311 (2007).

[56] T. Suda, private communications, 2013.

[57] Y. Kondo *et al.*, *Phys. Lett. B* **690**, 245 (2010).

[58] N. Kobayashi *et al.*, *Phys. Rev. C* **86**, 054604 (2012).

[59] Yu. Aksyutina *et al.*, *Phys. Lett. B* **718**, 1309 (2013).

[60] T. Uesaka, M. Sasano, private communications, 2015.